Letter

Diffusive density response of electrons in anisotropic multiband systems

Jeonghyeon Suh [1], Sunghoon Kim [1], E. H. Hwang [2,*] and Hongki Min [1,†]

[1] *Department of Physics and Astronomy, Seoul National University, Seoul 08826, Korea*

[2] *SKKU Advanced Institute of Nanotechnology and Department of Nano Engineering, Sungkyunkwan University, Suwon 16419, Korea*

(Received 7 February 2022; revised 11 August 2022; accepted 12 September 2022; published 23 September 2022)

We explicitly calculate the density-density response function with conserving vertex corrections for anisotropic multiband systems in the presence of impurities including long-range disorder. The direction dependence of the vertex corrections is correctly considered to obtain the diffusion constant which is given by a combination of componentwise transport relaxation times and velocities on the Fermi surface. We also investigate the diffusive density response of various anisotropic systems, propose some empirical rules for the corresponding diffusion constant, and demonstrate that it is crucial to consider the component dependence of the transport relaxation times to correctly interpret the transport properties of anisotropic systems, especially various topological materials with a different power-law dispersion in each direction.

DOI: 10.1103/PhysRevB.106.L121113

Introduction. Recently, many anisotropic or multiband systems, such as black phosphorus with a tunable band gap [1–9], nodal line semimetals [10–17], and multi-Weyl semimetals [18–26], have attracted much attention owing to their unique properties arising from their nodal structure with anisotropic nonlinear dispersion and the associated chiral nature of the wave functions. It is essential to understand how the anisotropy and multiband nature are manifested in the physical properties of these systems.

The fundamental transport properties in the presence of impurities can be understood from the diffusive dynamics of current and density fluctuations in response to the external fields. The former corresponds to the current response characterized by the dc conductivity, whose form in anisotropic multiband systems has been obtained through the semiclassical Boltzmann transport theory [27–30] or many-body diagrammatic theory [30]. On the other hand, the latter corresponds to the density response characterized by the diffusion constant. In isotropic single-band systems, the density response takes the form

$$\chi(\boldsymbol{q}, \nu) \sim \frac{1}{i\nu - \mathcal{D}q^2}, \tag{1}$$

which can be classically derived from the continuity equation $\frac{\partial \rho}{\partial t} + \nabla \cdot \boldsymbol{J} = 0$ and Fick's law $\boldsymbol{J} = -\mathcal{D}\nabla\rho$, where ρ, $\boldsymbol{J}$, and $\mathcal{D}$ are the number density, number current density, and diffusion constant, respectively. However, the diffusive density response of electrons in anisotropic multiband systems has not been exactly investigated in spite of its importance in understanding the corresponding diffusive transport. Thus, it is crucial to describe the density response correctly for anisotropic multiband systems in the presence of impurities.

In this Letter, using the diagrammatic approach we develop a theory to correctly evaluate the vertex corrections to the density-density response function and corresponding diffusion constant in anisotropic multiband systems in the presence of disorders, including long-range disorder, within the low impurity density limit. We incorporate the direction dependence of vertex corrections originating from the chirality and long-range disorder of the systems, and find that the diffusion constant is generally given by a nontrivial combination of componentwise transport relaxation times $\tau^{(i)}$ and velocities $v^{(i)}$ $(i = x, y, \ldots)$ on the Fermi surface, which satisfies the Einstein relation ensuring consistency with the continuity equation.

We use our results to calculate the diffusion constants of anisotropic two-dimensional electron gas (2DEG), anisotropic graphene, and few-layer black phosphorus (fBP) at the semi-Dirac transition point in the presence of long-range disorder for charged impurities. We demonstrate that the anisotropy of the diffusion constant (and also in the corresponding conductivity) strongly depends on the screening strength and deviates from the commonly expected anisotropy of the Fermi-velocity square, especially in highly anisotropic systems with a different power-law dispersion in each direction. Based on these observations, we propose some empirical rules for the anisotropy of the diffusion constant in anisotropic systems. We note that the anisotropy of the diffusion constant shows a significant difference from the one obtained neglecting the component dependence of the transport relaxation time, indicating that the component dependence of the transport relaxation time needs to be considered to correctly interpret the transport properties of anisotropic systems.

Vertex corrections to the density-density response function. Within the ladder vertex corrections (Fig. 1), we establish the density-density response function of a disordered electron gas with the charge vertex $\Lambda_{0\alpha}$ for band α as follows,

$$\chi(\boldsymbol{q}, i\nu_m) = \frac{\mathrm{g}}{\beta} \sum_{\alpha, i\omega_n} \int \frac{d^d k}{(2\pi)^d} \Lambda_{0\alpha}(\boldsymbol{k}, i\omega_n; \boldsymbol{q}, i\nu_m) \times \mathcal{G}_\alpha(\boldsymbol{k}, i\omega_n)\mathcal{G}_\alpha(\boldsymbol{k}+\boldsymbol{q}, i\omega_n + i\nu_m), \tag{2}$$

*euyheon@skku.edu
†hmin@snu.ac.kr

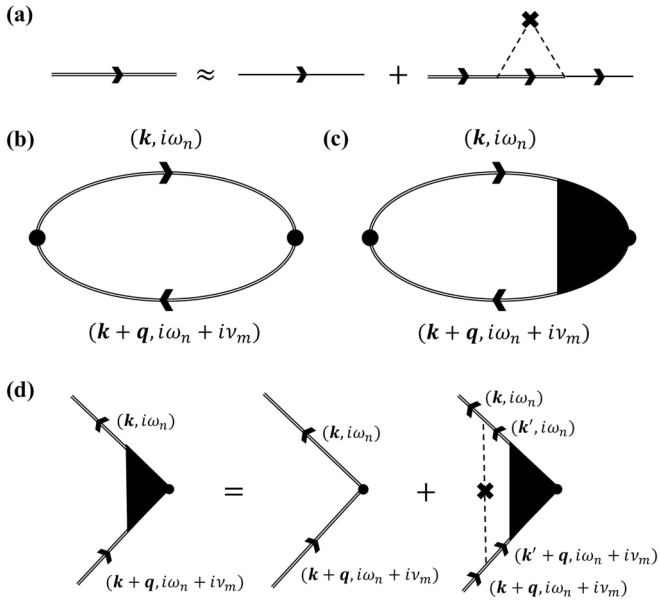

FIG. 1. Feynman diagrams for (a) the disorder-averaged Green's function within the Born approximation, (b) the density-density response function without vertex corrections, (c) the density-density response function with vertex corrections, and (d) the ladder approximation for the charge vertex.

where g is the spin/valley degeneracy factor, $\beta = 1/k_{\rm B}T$, and ω_n and ν_m are fermionic and bosonic Matsubara frequencies, respectively. Here, $\mathcal{G}_\alpha(\boldsymbol{k}, i\omega_n)$ is the disorder-averaged Green's function given by

$$\mathcal{G}_\alpha(\boldsymbol{k}, i\omega_n) = [i\omega_n - \xi_{\alpha,\boldsymbol{k}} - \Sigma_\alpha(\boldsymbol{k}, i\omega_n)]^{-1}, \tag{3}$$

where $\xi_{\alpha,\boldsymbol{k}}$ is the energy measured from the Fermi energy at state $(\alpha, \boldsymbol{k})$ and $\Sigma_\alpha(\boldsymbol{k}, i\omega_n)$ is the electron self-energy due to impurity scattering. Here, we assume a low temperature to ensure that the chemical potential can be approximated to the Fermi energy, and set $\hbar = 1$ for convenience.

Separating the charge vertex correction into two parts as $\Lambda_{0\alpha} = 1 + (\Lambda_{0\alpha} - 1)$, the density-density response function can be stated as $\chi = \chi_0 + \chi_1$. Here, χ_0 is the density-density response function without vertex corrections, whose leading order term for impurities in the static long-wavelength limit is given by $\chi_0 \approx -N(0)$ [see Sec. I of Supplemental Material [31]], where $N(\xi)$ is the density of states at energy ξ measured from the Fermi energy. Then, the contribution of the vertex corrections is given by

$$\chi_1(\boldsymbol{q}, i\nu_m) = \frac{\rm g}{\beta}\sum_{\alpha, i\omega_n}\int\frac{d^dk}{(2\pi)^d}[\Lambda_{0\alpha}(\boldsymbol{k}, i\omega_n; \boldsymbol{q}, i\nu_m) - 1] \times \mathcal{G}_\alpha(\boldsymbol{k}, i\omega_n)\mathcal{G}_\alpha(\boldsymbol{k}+\boldsymbol{q}, i\omega_n + i\nu_m). \tag{4}$$

We begin with considering the Dyson equation for the charge vertex $\Lambda_{0\alpha}$ within the ladder approximation [Fig. 1(d)] neglecting the quantum interference corrections,

$$\Lambda_{0\alpha}(\boldsymbol{k}, i\omega_n; \boldsymbol{q}, i\nu_m) = 1 + n_{\rm imp}\sum_{\alpha'}\int\frac{d^dk'}{(2\pi)^d}|V_{\alpha,\boldsymbol{k};\alpha',\boldsymbol{k}'}|^2\Lambda_{0\alpha'}(\boldsymbol{k}', i\omega_n; \boldsymbol{q}, i\nu_m) \times \mathcal{G}_{\alpha'}(\boldsymbol{k}', i\omega_n)\mathcal{G}_{\alpha'}(\boldsymbol{k}'+\boldsymbol{q}, i\omega_n + i\nu_m), \tag{5}$$

where $n_{\rm imp}$ is the impurity density and $V_{\alpha,\boldsymbol{k};\alpha',\boldsymbol{k}'}$ is the matrix element of the impurity potential between states $(\alpha, \boldsymbol{k})$ and $(\alpha', \boldsymbol{k}')$. In the long-wavelength limit where $\boldsymbol{q} \to \boldsymbol{0}$ and in the low frequency–low impurity density limit where ω_n and $\Sigma_\alpha(\boldsymbol{k}, i\omega_n)$ are negligible, Eq. (5) transforms into

$$\Lambda_{0\alpha}(\boldsymbol{k}, i\omega_n; \boldsymbol{q}, i\nu_m) - 1 \approx \Theta_{n,m}\sum_{\alpha'}\int\frac{d^dk'}{(2\pi)^d}W_{\alpha,\boldsymbol{k};\alpha',\boldsymbol{k}'}\frac{\Lambda_{0\alpha'}(\boldsymbol{k}', i\omega_n; \boldsymbol{q}, i\nu_m)}{\nu_m + i\boldsymbol{q}\cdot\boldsymbol{v}_{\alpha',\boldsymbol{k}'} + 1/\tau^{\rm qp}_{\alpha',\boldsymbol{k}'}}, \tag{6}$$

where $\Theta_{n,m} = 1$ for $-\nu_m < \omega_n < 0$ and 0 otherwise, $W_{\alpha,\boldsymbol{k};\alpha',\boldsymbol{k}'} \equiv 2\pi n_{\rm imp}|V_{\alpha,\boldsymbol{k};\alpha',\boldsymbol{k}'}|^2\delta(\xi_{\alpha,\boldsymbol{k}} - \xi_{\alpha',\boldsymbol{k}'})$ is the transition rate from state $(\alpha, \boldsymbol{k})$ to $(\alpha', \boldsymbol{k}')$, $\boldsymbol{v}_{\alpha,\boldsymbol{k}}$ is the velocity at $(\alpha, \boldsymbol{k})$, and $\tau^{\rm qp}_{\alpha,\boldsymbol{k}}$ is the quasiparticle lifetime for $(\alpha, \boldsymbol{k})$ which is given up to the first-order Born approximation [32] as

$$\frac{1}{\tau^{\rm qp}_{\alpha,\boldsymbol{k}}} = \sum_{\alpha'}\int\frac{d^dk'}{(2\pi)^d}W_{\alpha,\boldsymbol{k};\alpha',\boldsymbol{k}'}. \tag{7}$$

For detailed derivations, see Sec. II of Supplemental Material [31].

Similarly as in isotropic single-band systems [33], the charge vertex with $\boldsymbol{q} = \boldsymbol{0}$ for $(\alpha, \boldsymbol{k})$ on the Fermi surface is given by (see Sec. III of Supplemental Material [31])

$$\Lambda_{0\alpha}(\boldsymbol{k}, i\omega_n; \boldsymbol{0}, i\nu_m) = 1 + \frac{\Theta_{n,m}}{\nu_m\tau^{\rm qp}_{\alpha,\boldsymbol{k}}}. \tag{8}$$

Motivated from Eq. (8), we set an ansatz for the charge vertex as follows,

$$\Lambda_{0\alpha}(\boldsymbol{k}, i\omega_n; \boldsymbol{q}, i\nu_m) = 1 + \Theta_{n,m}\frac{1 - i\boldsymbol{q}\cdot\boldsymbol{l}_{\alpha,\boldsymbol{k}}}{\mathcal{V}_m(\boldsymbol{q}, \nu_m)\tau^{\rm qp}_{\alpha,\boldsymbol{k}}}, \tag{9}$$

for some $\boldsymbol{l}_{\alpha,\boldsymbol{k}}$ and $\mathcal{V}_m(\boldsymbol{q}, \nu_m)$ satisfying $\mathcal{V}_m(\boldsymbol{0}, \nu_m) = \nu_m$. The direction dependence of the charge vertex from the coupling between $\boldsymbol{q}$ and $\boldsymbol{k}$, which has been conventionally neglected to obtain a solution of the Dyson equation in a closed form [33,34], is considered up to linear order in $\boldsymbol{q}$ via the $\boldsymbol{q}\cdot\boldsymbol{l}_{\alpha,\boldsymbol{k}}$ term.

Inserting Eq. (9) into Eq. (6) and expanding the right-hand side in powers of $\boldsymbol{q}$ and ν_m, from the linear terms we obtain

$$l^{(i)}_{\alpha,\boldsymbol{k}} = v^{(i)}_{\alpha,\boldsymbol{k}}(\tau^{(i)}_{\alpha,\boldsymbol{k}} - \tau^{\rm qp}_{\alpha,\boldsymbol{k}}), \tag{10}$$

where $v^{(i)}_{\alpha,\boldsymbol{k}}$ and $\tau^{(i)}_{\alpha,\boldsymbol{k}}$ are the ith components of the velocity and transport relaxation time satisfying the following integral equation given by [27–30]

$$1 = \sum_{\alpha'}\int\frac{d^dk'}{(2\pi)^d}W_{\alpha,\boldsymbol{k};\alpha',\boldsymbol{k}'}\left(\tau^{(i)}_{\alpha,\boldsymbol{k}} - \frac{v^{(i)}_{\alpha',\boldsymbol{k}'}}{v^{(i)}_{\alpha,\boldsymbol{k}}}\tau^{(i)}_{\alpha',\boldsymbol{k}'}\right). \tag{11}$$

As seen in Eq. (10), the $\boldsymbol{q}\cdot\boldsymbol{l}_{\alpha,\boldsymbol{k}}$ term added to the conventional derivations vanishes only if the quasiparticle lifetime and transport relaxation time coincide, which occurs for nonchiral systems with short-range disorder. Thus, we infer that the $\boldsymbol{q}\cdot\boldsymbol{l}_{\alpha,\boldsymbol{k}}$ term originates from the chirality and long-range disorder of the systems. On the other hand, from the quadratic terms averaged over the Fermi surface we obtain

$$\mathcal{V}_m(\boldsymbol{q}, \nu_m) = \nu_m + \sum_{i,j}q_iq_j\mathcal{D}_{ij} + O^3(\boldsymbol{q}, \nu_m). \tag{12}$$

Here, $O^n(\boldsymbol{q}, \nu_m)$ represents the subleading terms of nth order or higher in $\boldsymbol{q}$ and ν_m, and $\mathcal{D}_{ij}$ is the diffusion constant defined by

$$\mathcal{D}_{ij} = \frac{1}{\tilde{N}(0)} \sum_{\alpha} \int \frac{d^d k}{(2\pi)^d} \delta(\xi_{\alpha,\boldsymbol{k}}) v^{(i)}_{\alpha,\boldsymbol{k}} v^{(j)}_{\alpha,\boldsymbol{k}} \tau^{(j)}_{\alpha,\boldsymbol{k}}, \tag{13}$$

where $\tilde{N}(\xi) \equiv N(\xi)/\mathrm{g}$ is the density of states per degeneracy at energy ξ. See Sec. IV of Supplemental Material [31] for the detailed derivations of Eqs. (10) and (12). Note that the diffusion constant in Eq. (13) is symmetric with respect to the indices i and j. Using Eq. (11), Eq. (13) can be rewritten as

$$\begin{aligned}\mathcal{D}_{ij} = {} & \frac{1}{\tilde{N}(0)} \sum_{\alpha} \int \frac{d^d k}{(2\pi)^d} \delta(\xi_{\alpha,\boldsymbol{k}}) v^{(i)}_{\alpha,\boldsymbol{k}} v^{(j)}_{\alpha,\boldsymbol{k}} \tau^{(i)}_{\alpha,\boldsymbol{k}} \tau^{(j)}_{\alpha,\boldsymbol{k}} \left(\tau^{\mathrm{qp}}_{\alpha,\boldsymbol{k}}\right)^{-1} \\ & - \frac{1}{\tilde{N}(0)} \sum_{\alpha,\alpha'} \int \frac{d^d k}{(2\pi)^d} \int \frac{d^d k'}{(2\pi)^d} W_{\alpha,\boldsymbol{k};\alpha',\boldsymbol{k}'} \\ & \times \delta(\xi_{\alpha,\boldsymbol{k}}) v^{(i)}_{\alpha,\boldsymbol{k}} v^{(j)}_{\alpha',\boldsymbol{k}'} \tau^{(i)}_{\alpha,\boldsymbol{k}} \tau^{(j)}_{\alpha',\boldsymbol{k}'}, \end{aligned} \tag{14}$$

which clearly reflects the symmetry with respect to the indices i and j.

Repeating the process in Sec. II of Supplemental Material [31], Eq. (4) can be rewritten as

$$\begin{aligned}\chi_1(\boldsymbol{q}, i\nu_m) = {} & \frac{2\pi\,\mathrm{g}}{\beta} \sum_{\alpha, i\omega_n} \Theta_{n,m} \int \frac{d^d k}{(2\pi)^d} \delta(\xi_{\alpha,\boldsymbol{k}}) \\ & \times \frac{\tau^{\mathrm{qp}}_{\alpha,\boldsymbol{k}} [\Lambda_{0\alpha}(\boldsymbol{k}, i\omega_n; \boldsymbol{q}, i\nu_m) - 1]}{1 + \nu_m \tau^{\mathrm{qp}}_{\alpha,\boldsymbol{k}} + i\boldsymbol{q} \cdot \boldsymbol{v}_{\alpha,\boldsymbol{k}} \tau^{\mathrm{qp}}_{\alpha,\boldsymbol{k}}}. \end{aligned} \tag{15}$$

Inserting Eq. (9) into Eq. (15) and expanding the right-hand side, we finally obtain

$$\chi_1(\boldsymbol{q}, i\nu_m) = N(0) \frac{\nu_m [1 + O^1(\boldsymbol{q}, \nu_m)]}{\nu_m + \sum_{i,j} q_i q_j \mathcal{D}_{ij} + O^3(\boldsymbol{q}, \nu_m)}. \tag{16}$$

Here, we have used $\frac{2\pi}{\beta} \sum_{i\omega_n} \Theta_{n,m} = \nu_m$. Therefore, up to leading order in $\boldsymbol{q}$ and ν_m, $\chi(\boldsymbol{q}, i\nu_m) = \chi_0(\boldsymbol{q}, i\nu_m) + \chi_1(\boldsymbol{q}, i\nu_m)$ is given by

$$\chi(\boldsymbol{q}, i\nu_m) \approx -N(0) \frac{\sum_{i,j} q_i q_j \mathcal{D}_{ij}}{\nu_m + \sum_{i,j} q_i q_j \mathcal{D}_{ij}}. \tag{17}$$

Through the analytic continuation $i\nu_m \to \nu + i0^+$, the retarded density-density response function is given by

$$\chi^{(\mathrm{R})}(\boldsymbol{q}, \nu) = N(0) \frac{\sum_{i,j} q_i q_j \mathcal{D}_{ij}}{i\nu - \sum_{i,j} q_i q_j \mathcal{D}_{ij}}. \tag{18}$$

For alternative derivations performing the frequency summation first, see Sec. V of Supplemental Material [31].

Evaluation of the diffusion constants in anisotropic systems. We evaluate the diffusion constants in anisotropic 2DEG, anisotropic graphene, and fBP at the semi-Dirac transition point for both short-range disorder and long-range disorder. For the anisotropy factor $A = k_{\mathrm{F}}^{(x)}/k_{\mathrm{F}}^{(y)}$ characterizing the anisotropy of the Fermi surface where $k_{\mathrm{F}}^{(i)}$ is the Fermi wave vector along the ith direction, we use $A = 2, 5$ estimated from fBP at the semi-Dirac transition point with a typical doping concentration $n = 10^{12}$–10^{13} cm^{-2}, whereas for anisotropic 2DEG and anisotropic graphene, we use the same A for comparison. See Sec. VI of Supplemental Material [31] for details.

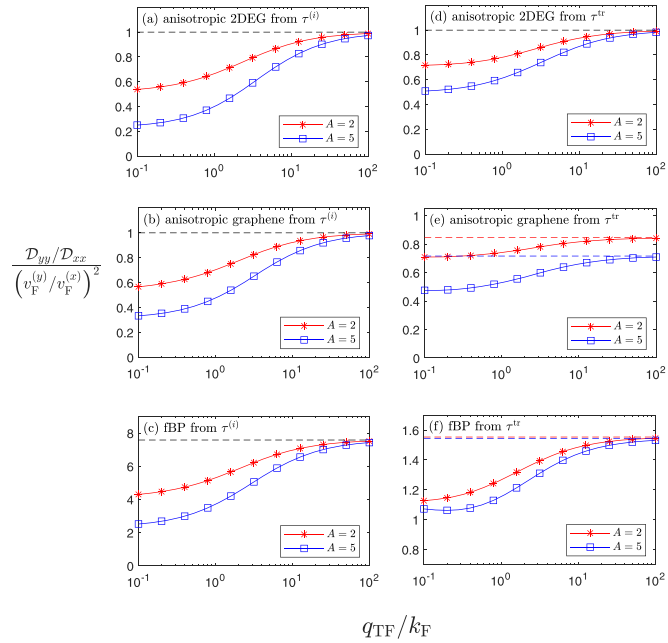

FIG. 2. Anisotropy $\mathcal{D}_{yy}/\mathcal{D}_{xx}$ of the diffusion constant normalized by $(v_{\mathrm{F}}^{(y)}/v_{\mathrm{F}}^{(x)})^2$ as a function of the screening factor Q for (a), (d) anisotropic 2DEG, (b), (e) anisotropic graphene, and (c), (f) fBP at the semi-Dirac transition point, obtained from (a)–(c) Eq. (13) considering the component dependence of the transport relaxation time and from (d)–(f) Eq. (19) neglecting the component dependence of the transport relaxation time as in isotropic systems. Here, $Q \equiv q_{\mathrm{TF}}/k_{\mathrm{F}}$ and $A \equiv k_{\mathrm{F}}^{(x)}/k_{\mathrm{F}}^{(y)}$. The values for the short-range disorder are represented by the dashed lines with the corresponding colors or by the black dashed lines if they coincide.

In anisotropic 2DEG and anisotropic graphene, $\mathcal{D}_{yy}/\mathcal{D}_{xx}$ is equal to the commonly expected $(v_{\mathrm{F}}^{(y)}/v_{\mathrm{F}}^{(x)})^2$ for short-range disorder, where $v_{\mathrm{F}}^{(i)}$ is the Fermi velocity along the ith direction, whereas for long-range disorder it deviates from $(v_{\mathrm{F}}^{(y)}/v_{\mathrm{F}}^{(x)})^2$ and depends on the screening factor $Q \equiv q_{\mathrm{TF}}/k_{\mathrm{F}}$ characterizing the screening strength, where q_{TF} is the Thomas-Fermi wave vector and k_{F} is the effective Fermi wave vector. In the strong screening limit, the result eventually approaches that of the short-range disorder [Figs. 2(a) and 2(b)]. In fBP at the semi-Dirac transition point where the energy dispersion is quadratic/linear along the zigzag (x)/armchair (y) direction with different power laws depending on the direction, $\mathcal{D}_{yy}/\mathcal{D}_{xx}$ becomes $7.6(v_{\mathrm{F}}^{(y)}/v_{\mathrm{F}}^{(x)})^2$ differing from $(v_{\mathrm{F}}^{(y)}/v_{\mathrm{F}}^{(x)})^2$ even for short-range disorder. For long-range disorder, it increases with the screening strength, approaching the short-range result in the strong screening limit [Fig. 2(c)]. Note that the dependence on the screening strength becomes larger as the anisotropy of the system increases for all cases [Figs. 2(a)–2(c)]. For detailed derivations and numerical calculations, see Sec. VI of Supplemental Material [31].

When the system has the same power-law dispersion in each direction as in anisotropic 2DEG and anisotropic graphene, for short-range disorder $\tau_{\boldsymbol{k}}^{(i)}$ becomes the same for

each component i and independent of the direction of $\boldsymbol{k}$ that $\mathcal{D}_{yy}/\mathcal{D}_{xx} = (v_{\rm F}^{(y)}/v_{\rm F}^{(x)})^2$. For long-range disorder, $\tau_{\boldsymbol{k}}^{(i)}$ has a dependence not only on the direction of $\boldsymbol{k}$ but also on i that the deviation of $\mathcal{D}_{yy}/\mathcal{D}_{xx}$ from $(v_{\rm F}^{(y)}/v_{\rm F}^{(x)})^2$ increases as the screening becomes weaker. When the system has a different power-law dispersion in each direction as in fBP at the semi-Dirac transition point, $\tau_{\boldsymbol{k}}^{(i)}$ has a dependence not only on the direction of $\boldsymbol{k}$ but also on the component i even for short-range disorder, yielding a significant deviation of $\mathcal{D}_{yy}/\mathcal{D}_{xx}$ from $(v_{\rm F}^{(y)}/v_{\rm F}^{(x)})^2$. In both cases, the deviation in anisotropy arising from $\tau_{\boldsymbol{k}}^{(i)}$ shows a stronger dependence on the screening compared to that obtained from

$$\frac{1}{\tau_{\boldsymbol{k}}^{\rm tr}} = \int \frac{d^d k'}{(2\pi)^d} W_{\boldsymbol{k};\boldsymbol{k}'}(1-\hat{\boldsymbol{k}}\cdot\hat{\boldsymbol{k}}'), \tag{19}$$

neglecting the dependence on the component i as in isotropic systems [Figs. 2(d)–2(f)]. From these observations, we find that the componentwise transport relaxation time should be considered to correctly interpret the transport properties of anisotropic systems, especially when dealing with highly anisotropic systems with a different power-law dispersion in each direction, even in the strong screening limit.

Furthermore, from the Einstein relation in anisotropic multiband systems [27–30], the dc conductivity is given by

$$\sigma_{ij}(\boldsymbol{q}\to\boldsymbol{0}) = e^2 N(0)\mathcal{D}_{ij}, \tag{20}$$

thus we have $\sigma_{yy}/\sigma_{xx} = \mathcal{D}_{yy}/\mathcal{D}_{xx}$. Consequently, the anisotropy of the conductivity also shows a significant difference from that estimated neglecting the component dependence of transport relaxation time for long-range disorder, and even for short-range disorder when the system has a different power-law dispersion in each direction.

Discussion. In d-dimensional isotropic single-band systems, the diffusion constant in Eq. (13) reduces to

$$\mathcal{D} = \frac{v_{\rm F}^2 \tau^{\rm tr}}{d}, \tag{21}$$

which has the same form appearing in the Einstein relation. However, the conventional many-body diagrammatic approach considering the vertex corrections to the density-density response function gives the diffusion constant to be [33,34]

$$\mathcal{D} = \frac{v_{\rm F}^2 \tau^{\rm qp}}{d}, \tag{22}$$

where $\tau^{\rm qp}$ is the quasiparticle lifetime. The difference between the conventional approach and our results originates from the additional $\boldsymbol{q}\cdot\boldsymbol{l}_{\boldsymbol{k}}$ term in Eq. (9), which is the only direction dependence on $\boldsymbol{q}$ for isotropic systems. As mentioned, the conventional approach in isotropic single-band systems neglects the direction dependence of the charge vertex to obtain a solution of the Dyson equation in a closed form. However, the Dyson equation in Eq. (5) actually depends on the direction of $\boldsymbol{q}$ through the $\boldsymbol{k}$ dependence in $W_{\alpha,\boldsymbol{k};\alpha',\boldsymbol{k}'}$ when the system has chirality or long-range disorder. We correctly considered this direction dependence in the Dyson equation and obtain the corresponding solutions up to linear order in $\boldsymbol{q}$, and to quadratic order in $\boldsymbol{q}$ averaged over the Fermi surface, respectively.

Furthermore, the diffusion constant given by Eq. (13) correctly describes the diffusive dynamics. From the continuity equation $\frac{\partial\rho}{\partial t} + \boldsymbol{\nabla}\cdot\boldsymbol{J} = 0$, the density-density response function and conductivity are related as $i\nu e^2\chi(\boldsymbol{q},\nu) + \sum_{i,j}\sigma_{ij}q_i q_j = 0$. Thus, using $\chi(\boldsymbol{q}\to\boldsymbol{0},\nu) \approx N(0)\sum_{i,j} q_i q_j \mathcal{D}_{ij}/i\nu$ from Eq. (18), we can reproduce the Einstein relation in Eq. (20).

In disordered systems, the density-density response function has the diffusion pole presenting a pronounced peak at low frequencies in the density fluctuation spectrum, which affects the quasiparticle properties of a disordered electron liquid [36]. In anisotropic multiband systems, the density-density response function is given by Eq. (18) characterized by the diffusion pole structure, thus the diffusion pole occurs at $\nu = -i\sum_{i,j} q_i q_j \mathcal{D}_{ij}$. Since the diffusion constant given by Eq. (13) is anisotropic in general, the diffusion pole occurring due to disorder may affect the quasiparticle properties anisotropically. Thus, studying the anisotropy of the diffusion constant correctly considering the component dependence of the transport relaxation time is important to understand the effect of disorder in anisotropic multiband systems.

In summary, using a many-body diagrammatic approach, we develop a theory for the vertex corrections to the density-density response function and find the corresponding diffusion constant in anisotropic multiband systems. We fully incorporate the direction dependence of the charge vertex, especially the one from the chirality and long-range disorder of the systems, and find that the diffusion constant obtained in this many-body diagrammatic approach is associated with the componentwise transport relaxation time rather than the quasiparticle lifetime. This nontrivial result correctly describes the diffusive dynamics of anisotropic multiband systems, consistent with the continuity equation. Furthermore, we calculate the diffusion constants of various anisotropic systems in the presence of the long-range disorder for charged impurities and find that the inclusion of the component-dependent transport relaxation time is crucial to correctly describe the transport properties of anisotropic systems.

ACKNOWLEDGMENTS

This work was supported by the National Research Foundation of Korea (NRF) grant funded by the Korea government (MSIT) (Grant No. 2018R1A2B6007837) and Creative-Pioneering Researchers Program through Seoul National University (SNU). E.H. acknowledges support from Korea NRF (Grant No. 2021R1A2C1012176).

[1] F. Xia, H. Wang, J. C. M. Hwang, A. H. Castro Neto, and L. Yang, Black phosphorus and its isoelectronic materials, Nat. Rev. Phys. **1**, 306 (2019).

[2] F. Xia, H. Wang, and Y. Jia, Rediscovering black phosphorus as an anisotropic layered material for optoelectronics and electronics, Nat. Commun. **5**, 4458 (2014).

[3] J. Qiao, X. Kong, Z.-X. Hu, F. Yang, and W. Ji, High-mobility transport anisotropy and linear dichroism in few-layer black phosphorus, Nat. Commun. **5**, 4475 (2014).

[4] V. Tran, R. Soklaski, Y. Liang, and L. Yang, Layer-controlled band gap and anisotropic excitons in few-layer black phosphorus, Phys. Rev. B **89**, 235319 (2014).

[5] J. Kim, S. S. Baik, S. H. Ryu, Y. Sohn, S. Park, B.-G. Park, J. Denlinger, Y. Yi, H. J. Choi, and K. S. Kim, Observation of tunable bandgap and anisotropic Dirac semimetal state in black phosphorus, Science **349**, 723 (2015).

[6] S. S. Baik, K. S. Kim, Y. Yi, and H. J. Choi, Emergence of two-dimensional massless Dirac fermions, chiral pseudospins, and Berry's phase in potassium doped few-layer black phosphorus, Nano Lett. **15**, 7788 (2015).

[7] L. Li, F. Yang, G. J. Ye, Z. Zhang, Z. Zhu, W. Lou, X. Zhou, L. Li, K. Watanabe, T. Taniguchi, K. Chang, Y. Wang, X. H. Chen, and Y. Zhang, Quantum Hall effect in black phosphorus two-dimensional electron system, Nat. Nanotechnol. **11**, 593 (2016).

[8] J. Kim, S. S. Baik, S. W. Jung, Y. Sohn, S. H. Ryu, H. J. Choi, B.-J. Yang, and K. S. Kim, Two-Dimensional Dirac Fermions Protected by Space-Time Inversion Symmetry in Black Phosphorus, Phys. Rev. Lett. **119**, 226801 (2017).

[9] J. Jang, S. Ahn, and H. Min, Optical conductivity of black phosphorus with a tunable electronic structure, 2D Mater. **6**, 025029 (2019).

[10] C. Fang, H. Weng, X. Dai, and Z. Fang, Topological nodal line semimetals, Chin. Phys. B **25**, 117106 (2016).

[11] C. Fang, Y. Chen, H.-Y. Kee, and L. Fu, Topological nodal line semimetals with and without spin-orbital coupling, Phys. Rev. B **92**, 081201(R) (2015).

[12] Y. Huh, E.-G. Moon, and Y. B. Kim, Long-range Coulomb interaction in nodal-ring semimetals, Phys. Rev. B **93**, 035138 (2016).

[13] S. E. Han, G. Y. Cho, and E.-G. Moon, Topological phase transitions in line-nodal superconductors, Phys. Rev. B **95**, 094502 (2017).

[14] S. Ahn, E. J. Mele, and H. Min, Electrodynamics on Fermi Cyclides in Nodal Line Semimetals, Phys. Rev. Lett. **119**, 147402 (2017).

[15] W. B. Rui, Y. X. Zhao, and A. P. Schnyder, Topological transport in Dirac nodal-line semimetals, Phys. Rev. B **97**, 161113(R) (2018).

[16] W. Chen, H.-Z. Lu, and O. Zilberberg, Weak Localization and Antilocalization in Nodal-Line Semimetals: Dimensionality and Topological Effects, Phys. Rev. Lett. **122**, 196603 (2019).

[17] Y. Shao, A. N. Rudenko, J. Hu, Z. Sun, Y. Zhu, S. Moon, A. J. Millis, S. Yuan, A. I. Lichtenstein, D. Smirnov, Z. Q. Mao, M. I. Katsnelson, and D. N. Basov, Electronic correlations in nodal-line semimetals, Nat. Phys. **16**, 636 (2020).

[18] N. P. Armitage, E. J. Mele, and A. Vishwanath, Weyl and Dirac semimetals in three-dimensional solids, Rev. Mod. Phys. **90**, 015001 (2018).

[19] C. Fang, M. J. Gilbert, X. Dai, and B. A. Bernevig, Multi-Weyl Topological Semimetals Stabilized by Point Group Symmetry, Phys. Rev. Lett. **108**, 266802 (2012).

[20] P. E. C. Ashby and J. P. Carbotte, Chiral anomaly and optical absorption in Weyl semimetals, Phys. Rev. B **89**, 245121 (2014).

[21] S. Ahn, E. H. Hwang, and H. Min, Collective modes in multi-Weyl semimetals, Sci. Rep. **6**, 34023 (2016).

[22] S. Ahn, E. J. Mele, and H. Min, Optical conductivity of multi-Weyl semimetals, Phys. Rev. B **95**, 161112(R) (2017).

[23] S. E. Han, C. Lee, E.-G. Moon, and H. Min, Emergent Anisotropic Non-Fermi Liquid at a Topological Phase Transition in Three Dimensions, Phys. Rev. Lett. **122**, 187601 (2019).

[24] T. Nag, A. Menon, and B. Basu, Thermoelectric transport properties of Floquet multi-Weyl semimetals, Phys. Rev. B **102**, 014307 (2020).

[25] Z. Ning, B. Fu, Q. Shi, and X. Wang, Effect of weak disorder in multi-Weyl semimetals, Chin. Phys. B **29**, 077202 (2020).

[26] L. X. Fu and C. M. Wang, Thermoelectric transport of multi-Weyl semimetals in the quantum limit, Phys. Rev. B **105**, 035201 (2022).

[27] R. S. Sorbello, Anisotropic relaxation times for impurity scattering on the Fermi surface, J. Phys. F: Met. Phys. **4**, 1665 (1974).

[28] Y. Liu, T. Low, and P. P. Ruden, Mobility anisotropy in monolayer black phosphorus due to scattering by charged impurities, Phys. Rev. B **93**, 165402 (2016).

[29] S. Park, S. Woo, E. J. Mele, and H. Min, Semiclassical Boltzmann transport theory for multi-Weyl semimetals, Phys. Rev. B **95**, 161113(R) (2017).

[30] S. Kim, S. Woo, and H. Min, Vertex corrections to the dc conductivity in anisotropic multiband systems, Phys. Rev. B **99**, 165107 (2019).

[31] See Supplemental Material at http://link.aps.org/supplemental/10.1103/PhysRevB.106.L121113 for the detailed derivations of the charge vertex, alternative derivations for the vertex corrections, and calculations for the diffusion constants, which includes Refs. [2,9,29,30,32–35,37–40].

[32] H. Bruus and K. Flensberg, *Many-Body Quantum Theory in Condensed Matter Physics* (Oxford University Press, Oxford, U.K., 2004).

[33] P. Coleman, *Introduction to Many-Body Physics* (Cambridge University Press, Cambridge, U.K., 2016).

[34] P. Brouwer, Theory of Many-Particle Systems, Lecture Notes for P654, Cornell University, Spring 2005 (unpublished).

[35] J. R. Schrieffer, *Theory of Superconductivity* (Benjamin, New York, 1964).

[36] G. F. Giuliani and G. Vignale, *Quantum Theory of the Electron Liquid* (Cambridge University, Cambridge, U.K., 2005).

[37] G. D. Mahan, *Many-Particle Physics* (Springer, Berlin, 2000).

[38] S. Park, S. Woo, and H. Min, Semiclassical Boltzmann transport theory of few-layer black phosphorous in various phases, 2D Mater. **6**, 025016 (2019).

[39] M. L. Boas, *Mathematical Methods in the Physical Science* (Wiley, New York, 2006).

[40] D. Xiang, C. Han, J. Wu, S. Zhong, Y. Liu, J. Lin, X.-A. Zhang, W. P. Hu, B. Özyilmaz, A. H. Castro Neto, A. T. S. Wee, and W. Chen, Surface transfer doping induced effective modulation on ambipolar characteristics of few-layer black phosphorus, Nat. Commun. **6**, 6485 (2015).